Journal of Nano- and Electronic Physics
Vol. **17** No 4, 04036(6pp) (2025)

Журнал нано- та електронної фізики
Том **17** № 4, 04036(6cc) (2025)

OPEN ACCESS

REGULAR ARTICLE

Gadolinium Nanoparticles: A Promising Agent for Enhancing Radiotherapy at Low Concentrations

L. Benabed[1,*], A.S.A. Dib[1], A. Djelloul[2,†]

[1] *Departement of Physics, Faculty of Physics, Laboratory of Analysis and Application of Radiation, Université des Sciences et de la Technologie d'Oran Mohamed Boudiaf, USTO-MB, BP 1505 EL M'naouer, 31000 Oran, Algeria*
[2] *Centre de Recherche en Technologie des Semi-Conducteurs pour l'Energétique 'CRTSE', 02 Bd Frantz Fanon, BP 140, 7 Merveilles, Alger, Algérie*

(Received 25 April 2025; revised manuscript received 22 August 2025; published online 29 August 2025)

Over the last few years, nanomedicine has made significant progress. Nanoparticles are currently being introduced into tumors to enhance treatment, increase the efficiency of drug delivery to tumors, and reduce the toxicity of cancer treatments. The goal of this work is to investigate the improvement of a deep tumor in the center of the human head by radiotherapy, in which nanomaterials were injected in low quantities. Using the Monte Carlo Geant4 code, we built a geometry of a human head in which we placed a spherical tumor with a diameter of 1.3 cm. We are interested in researching the effect of biocompatible nanomaterials added to tumors during X-ray radiotherapy. We focused on the most well-known biocompatible nanomaterials utilized in nanomedicine, including gadolinium (GdNPs), platinum (PtNPs), silver (SvNPs), and gold (AuNPs), particularly at low concentrations. Our findings demonstrate that, in comparison to other nanomaterials, the presence of GdNPs inside the tumor offers the greatest dose absorption at the tumor level upon exposure to 60 keV X-ray radiation, with a performance of 37 %. In comparison to the best-known materials in the literature, such as gold and platinum, our Monte Carlo simulation demonstrates that gadolinium nanoparticles have a high efficiency at low concentrations.

Keywords: Radiation dose, Nanomaterials, Auger effect, Tumor Dose Absorption, 3D surface topography.

DOI: 10.21272/jnep.17(4).04036

PACS numbers: 07.85.Qe, 71, 79.20.Fv, 78.40.Ri, 91.10.Jf

1. INTRODUCTION

With the growth of nanomedicine, the fabrication of bionanomaterials (bio-NMS) is becoming increasingly advanced, as a result the use of bio-NMS has become one of the most promising strategies in the treatment of cancer [1, 2]. Indeed, numerous recent studies have demonstrated that incorporating bio-NMS into a tumor increases early detection and imaging [3] and leads to improved treatments [4].

High-Z materials can increase the dosage of ionizing radiation by enhancing the photoelectric effect; gold is the most commonly studied substance. Herold et al, 2000 [5] originally demonstrated that when subjected to kilovoltage photon beams, gold microspheres suspended in cell cultures or dispersed in tumor tissues can yield a higher physiologically effective dosage. Later, Hainfeld et al. 2004 [6] revealed that gold nanoparticles (AuNPs) administered intravenously into mice with subcutaneous EMT-6 mammary carcinomas improved 250 kVp X-ray irradiation. Connor et al. 2005 [7] investigated the absorption and toxicity of 18 nm diameter gold nanoparticles in human leukemia cells, concluding that gold nanoparticles do not impair cellular activity. Brun et al. [8] revealed that the radiosensitizing effect of AuNPs is enhanced when the Gold:DNA ratio increases, as a result, AuNPs subjected to X-Ray radiation appear to be a potential tool for anti-microbial proliferation or the elimination of undesirable bacteria. Another alternative to gold nanoparticles is gadolinium (Gd, Z = 64). In addition to having a relatively high atomic number, Gd is already utilized as a contrast agent in MRI. Gd is used in admixture with other soluble materials because it is stable and non-toxic. Recently, the accumulation of Gd-based contrast agents has been demonstrated in various organs such as the kidneys, liver and nervous system. Shikata et al. 2002 [9] studied in vitro the accumulation of gadolinium in tumor cells and reached a concentration of 40 ppm. Hebert E.M et al. 2010 [10] studied the radiosensitization of gold nanoparticles coated with Gd in vitro in mice. They observed a preferential accumulation of gold in tumors with significant toxicity for tumor cells in vitro, but no obvious toxicity for mice. Gd_2O_3 core nanoparticles encased in a polysiloxane shell showed potential as an image-guided radiotherapeutic tool in a gliosarcoma rat model [11]. MRI revealed the accumulation of nanoparticles in the tumor after vein injection, and tumor animals were treated with microbeam radiation, which resulted in a considerable rise. Another study, employing a rat brain tumor model, showed that

* Correspondence e-mail: lahouari.benabed@univ-usto.dz
† djelloulcrtse@gmail.com

Cite this article as: L. Benabed et al., *J. Nano- Electron. Phys.* 17 No 4, 04036 (2025) https://doi.org/10.21272/jnep.17(4).04036

after IV administration, Gd-based nanoparticles assemble in brain tumors [12]. Several researchers have been interested in gadolinium in vitro and in vivo [13-16]. According to recent work by Pavlína et al. 2020 [17], in vivo, no Gd-lip cytotoxicity was observed up to 72 hours of exposure in human liver cancer cells with a Gd concentration varying between 1 μM and 100 μM. These results make nanomedicine researchers interested in gadolinium-based nanomaterials. In this field, the application of the Monte Carlo code in radiotherapy has been validated by several researchers [18], Autumn et al. 2016 [19] confirmed that the Monte Carlo simulation is the best choice to evaluate the increase in dose with nanoparticles in radiotherapy. In addition, Noblet et al. 2018 [20], calculated the deep dose and confirmed a good correlation between simulations and measurements, with uncertainties estimated at 1 %.

In this study, we used the Monte Carlo code Geant4 to optimize radiation for a deep brain tumor, particularly when there are low concentrations of nanomaterials present in the tumor during radiation. Our main goal is to reduce the toxicity and adverse effects of these nanomaterials while increasing the dose absorbed in the tumor. The main challenge for this type of tumor is breaking through the hematoencephalic barrier, which allows access to essential nutrients but blocks access to other substances. As a result, several teams are working on effective drug delivery methods in the field [21, 22]. We have a particular focus on biocompatible nanomaterials, which are frequently used in nanomedicine studies, such as gold (AuNPs) [23], platinum (PtNPs) [24], silver (SvNPs) [25], and gadolinium (GdNPs) [26-28].

This study is novel in several ways. It may offer a number of advantages, such as more efficient drug delivery to tumors, less toxicity from cancer treatments, and better treatment for brain tumors.

2. EXPERIMENTAL DETAILS

2.1 Simulation of a Tumor Inside a Human Head

We propose to use Geant4 Monte Carlo [29, 30] to simulate radiotherapy of a spherical tumor in the center of an adult-sized head. Our goal is to observe the impact of bio-NMs on the tumor's ability to absorb the dose, especially in the case of a very low concentration of 20 ppm. (see Figure1).

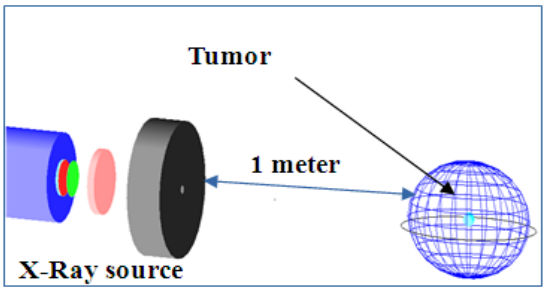

Fig. 1 – Monte Carlo simulation of X-ray exposure of a human head phantom. The radiation source is one meter away from the head. The radiation beam's energy ranged from 20 to 200 keV in 10 keV steps for each simulation

To achieve more precise results, we used a low electromagnetic [31, 32] energy package with a cutoff energy of 250 eV and a step size of 1 nm. As mentioned previously, our goal was to determine the absorbed dose in the tumor both in the presence and absence of nanoparticles. We constructed the geometry of an adult head and inserted a 1.5 cm-diameter spherical tumor into the center of the head. The head and tumor assembly are exposed to a monoenergetic X-ray whose energy varies from 20 keV to 200 keV in 10 keV steps for each simulation. This X-ray is one meter away from the patient. As already mentioned, our goal was to determine the dose absorbed by the tumor in the presence and absence of nanoparticles. As a result, we created the geometry of an adult head, including all of its material constituents. The human head geometry is primarily composed of a 0.8 cm thick skull and brain tissue. The skeleton is then covered with 0.2 cm thick soft tissue. A 1.5 cm diameter spherical tumor was built in the middle of the head. The Geant4 database is used to obtain the chemical compositions and densities of the skeleton, brain, soft tissues, and tumors (see Table 1).

Table 1 – The chemical compositions of each material that makes up the human head, expressed as a percentage of mass [33]

Material and density	O	C	H	N	Na	Mg	P	S	Cl	K	Ca
Scalp ($1.09\ g\ cm^{-3}$)	61.8	20.4	10	4.2	0.2	-	0.1	0.2	0.3	0.1	-
Skeleton ($1.61g\ cm^{-3}$)	40.8	21.2	5	4	0.1	0.2	8.1	0.3	-	-	17.6
Brain ($1.040\ g\ cm^{-3}$) and Tumor ($1.14g\ cm^{-3}$)	68.5	14.5	10.7	2.2	0.2	-	0.40	0.2	0.3	0.3	-

3. RESULTS AND DISCUSSION

3.1 Simulation of a Tumor Inside a Human Head

The plot of the absorbed energy in the skull after exposure to 90 keV of X-rays is shown in Figure 2. In this case, a patient's head is exposed to an X-ray source that is positioned one meter away. We employed the low electromagnetic energy package with a cut-off energy of 250 eV and a step range of 0.1 um in this simulation part. The 109 gamma rays were released in the z-axis direction from the radiation source in order to acquire data with a high degree of accuracy; the calculating process took more than three days on a 12-node HP workstation. The Monte Carlo approach, as is widely known, yields approximate results [34].

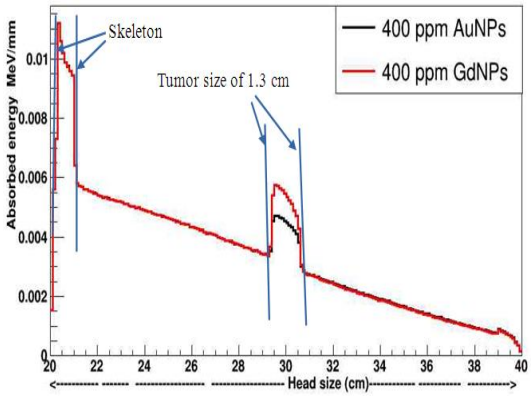

Fig. 2 – The energy absorbed in the head during 90 keV X-ray beam head irradiation. In the case of the presence of GdNPs or AuNPs with concentrations of 400 ppm. The tumor is located in the center of the brain

With the implantation of bio-NMs into the tumor, as seen in this image, the absorbed dose rises significantly. In fact, 400 ppm AuNPs (or GdNPs) increase the amount of dosage that is absorbed. GdNPs, as observed, enhance the absorbed dose in tumor more than AuNPs. This finding does not contradict existing research, which argues that gold is the greatest dose potentiator in radiotherapy.

Indeed, in our investigation, we employed the mass quantity of nanomaterials delivered into the tumor rather than the fraction of these nanomaterials in relation to the size of the tumor.

Table 2 – The percentage corresponding to the mass of 20 ppm for each type of material injected into the 1.3 cm diameter spherical tumor

20 ppm of nanomaterials	Equivalent percentage in relation to the tumor's volume
Gold nanoparticles (AuNPs)	0.1094%
Platinum nanoparticles (PtNPs)	0.098 %
Silver nanoparticles (SvNPs)	0.21139%
Gadolinium nanoparticles (GdNPs)	0.2915%

According to Table 2, a quantity of 20 ppm Gadolinium takes up three times the space as the same amount of Gold mass in a 1.3 cm diameter spherical tumor, which explains why Gadolinium absorbs more than Gold.

3.2 Dose Absorption Ratio

The R value in equation (1) represents the dose absorption ratio (DAR) between the absorbed dose within the tumor in the presence of nanoparticles and the absorbed dose without nanoparticles. The DAR value describes the direct effect of nanoparticles on absorbed dose during radiotherapy. Figure 3 illustrates the computed dose ratio R in the tumor caused by the addition of various NMs at the same concentration of 20 ppm and during exposure to X-rays with energies ranging from 20 to 250 keV.

$$R=\frac{\text{Tumor Absorbed Dose with NPs}}{\text{Tumor Absorbed Dose without NPs}} \qquad (1)$$

The trace of the dose absorbed ratio R in the tumor with the addition of GdNPs reveals two peaks, the first at 40 keV and the second at 60 keV, as shown in Figure 3. The first maximum's absorbed dose ratio R has grown by 21 %, while the second has increased by 37 %. In the case of SvNPs, there is a single maximum at 50 keV with a 28 % increase in R.

It should be noted that with a concentration of AuNPs and PtNPs equivalent to GdNPs and SvNPs, the R value increases slightly. In fact, they do reach their maximums at 50 keV for AuNPs and 40 keV for PtNPs, respectively, with an absorbed dose ratio R of 15 % and 14 %. Our findings support the experimental findings and Monte Carlo simulations of Santibanez et al. 2018 [35], who found a considerable improvement in dosage in the presence of gadolinium of up to 253 %.

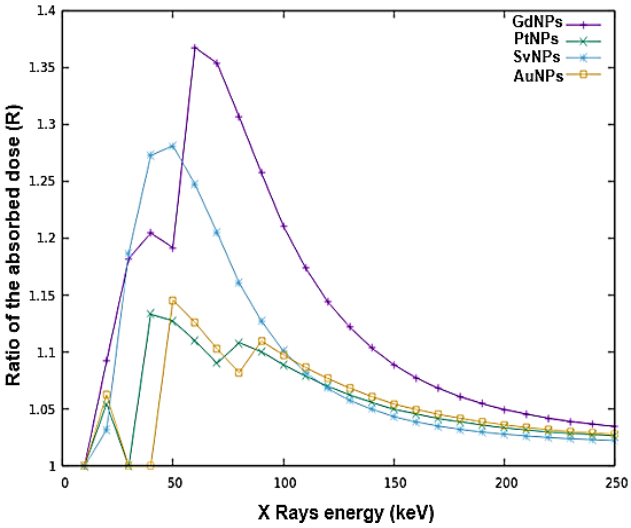

Fig. 3 – Plots of the dose absorbed ratio R within the tumor versus the X-ray energy (ranging from 10 keV to 250 keV) for different types of bio-NPs with a 20 ppm concentration. The tumor is localized within the brain

3.3 Auger-electrons Spectrum

The Auger effect is the primary physical phenomenon that occurs when X-rays interact with nanoparticles made up of heavy atoms [36]. This process occurs when an electron absorbs energy from an X-ray photon, resulting in its ejection from the atom's inner electron shell and creating a hole. When an electron from a higher energy level fills this hole, it generates a photon known as X-ray Fluorescence. To further understand the results in Figure 3, we are particularly interested in the computation of Auger electrons at the tumor exit during an external exposure of the phantom head with an X-ray energy of 60 keV.

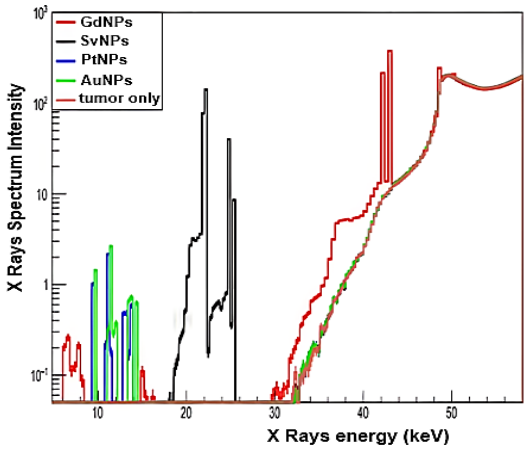

Fig. 4 – X-ray spectrum intensity for different types of bio-NPs with a 20 ppm concentration. The tumor is localized within the brain, X-ray energy of 60 keV

Figure 4 depicts the spectrum of Auger electrons for each type of metallic nanoparticle. Two intense Auger electron peaks with energies about 42 keV and 44 keV are clearly seen when GdNPs are present, as opposed to SvNPs, which produce a spectrum in the energy range of 18 keV to 26 keV. AuNPs and PtNPs generate significantly fewer Auger electrons compared to GdNPs or

SvNPs. According to Figure 4, metallic nanoparticles improve the absorbed dose by ejecting secondary electrons (Auger electrons) and X-ray fluorescence. In fact, Gadolinium exhibits the greatest improvement upon exposure to an X-ray with an energy of 60 keV among the nanometals used in this study.

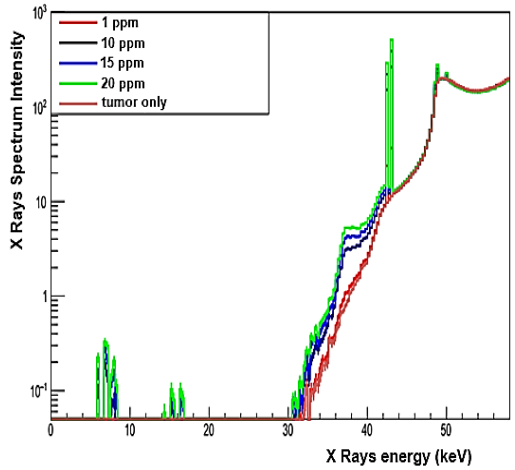

Fig. 5 – X-ray spectrum intensity for different concentration of GdNPs. The tumor is localized within the brain. X-ray energy of 60 keV

Figure 5 shows the Auger electron spectrum for various GdNPs concentrations ranging from 1 ppm to 20 ppm and for an X-ray energy of 60 keV. This figure shows that the Auger spectrum becomes increasingly significant as GdNPs concentration increases, especially above a concentration of 10 ppm; this quantity of GdNPs corresponds to 0.14 % of the overall tumor volume. The rise in the absorbed dose ratio R caused by Auger electrons produced by low quantities of GdNPs ranging from 1 ppm to 20 ppm is depicted in Figure 6. It should be noted that an increase in the absorbed dose R of up to 25 % may typically be achieved with only 10 ppm of GdNPs.

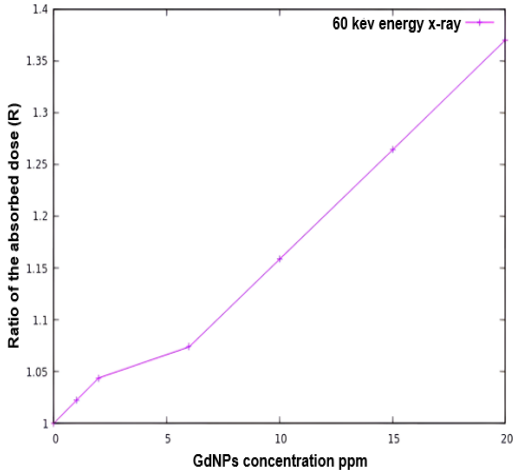

Fig. 6 – Calculation of the dose absorbed ratio R for different concentrations of GdNPs in an X-ray exposure of 60 keV of energy. The tumor is located in the brain

4. DISCUSSION

Several scientific investigations, including Monte Carlo simulations and both in vitro and in vivo animal experiments, have demonstrated that the presence of nanoparticles in a tumor enhances radiation absorption. However, no human patients have been treated thus far [37, 38]. Before commencing this new treatment procedure in the clinical setting, it is vital to understand the risks and negative consequences of these nanomaterials on human health. We used the same amount of bio-NPs in the tumor during X-ray exposure. In Figure 2, we show the absorbed dose along the head for the case of GdNPs and AuNPs with a concentration of 400 ppm added to the tumor. This figure makes it very evident that the presence of NPs has improved dose absorption at the tumor level. Furthermore, compared to AuNPs, GdNPs have superior dose absorption within the tumor. Because Gadolinium is a very good competitor compared to Gold, this result can be very helpful for researchers in the experimental field, whether they are working in vivo or in vitro. Our primary goal is to investigate the effects of well-known bioNPs such as AuNPs, PtNPs, SvNPs, and GdNPs at low concentrations; we selected a bio-NPs concentration of 20 ppm. According to the results shown in Figure 3, GdNPs improve tumor dose absorption the most, with an increase in the absorbed dose ratio R of up to 37 %, followed by SvNPs, which have an absorbed dose ratio R of around 28 % and AuNPs (respectively PtNPs), which has an increase of around 15 % (respectively 13 %). We were interested in studying the energy spectrum of Auger electrons caused by bio-NPs present in the tumor to better understand previous results. Following Figure 4, with an X-ray energy exposure of 60 keV, the energetic spectrum of Auger electrons contains two significant peaks around 42 and 44 keV, and when compared to other bio-NPs, the Auger electrons due to GdNPs are the most energetic, resulting in the greatest ranges and a significant increase in absorbed dose. On the other hand, we tracked the effect of different GdNP concentrations ranging from 1 ppm to 20 ppm while remaining within a small concentration range, and we found that increasing the GdNP concentration yielded the same two pics of energy around 22 and 44 keV but with a higher number of Auger electrons.

5. CONCLUSIONS

When compared to other known bio-NMs such as AuNPs, PtNPs, and SvNPs, our findings show that radiation performed in the presence of GdNPs is the most effective. Furthermore, appropriate X-ray energy in the energy range of 40 keV to 100 keV should be used to increase the dosage absorbed by a tumor. According to our modeling results, a concentration of 20 ppm gadolinium increases irradiation of deep brain tumors by 37 %.

AKNOWLEDGEMENTS

The authors would like to thank the General Directorate for Scientific Research and Technological Development (DGRST).

REFERENCES

1. C.N. Lok, T. Zou, J.J. Zhang, I.W.S. Lin, C.M. Che. *Adv. Mater.* **26** No 31, 5550 (2014).
2. H.M. Abdel-Mageed, N.Z. AbuelEzz, R.A. Radwan, S.A. Mohamed, *J. Microencapsul.* **38** No 6, 414 (2021).
3. J.C. Hsu, L.M. Nieves, O. Betzer, T. Sadan, P.B. Noël, R. Popovtzer, D.P. Cormode, *Wiley Interdiscip. Rev.: Nanomed. Nanobiotechnol.* **12** No 6, e1642 (2020).
4. R. Wang, J. Deng, D. He, E. Yang, W. Yang, D. Shi, Y. Jiang, Z. Qiu, T.J. Webster, Y. Shen, *Nanomedicine: Nanotechnology, Biology and Medicine* **16**, 195 (2019).
5. D.M. Herold, I.J. Das, C.C. Stobbe, R.V. Iyer, J.D. Chapman, *Int. J. Radiat. Biol.* **76** No 10, 1357 (2000).
6. J.F. Hainfeld, D.N. Slatkin, H.M. Smilowitz, *Phys. Med. Biol.* **49** No 18, N309 (2004).
7. E.E. Connor, J. Mwamuka, A. Gole, C.J. Murphy, M.D. Wyatt, *Small* **1** No 3, 325 (2005).
8. E. Brun, A. Simon-Deckers, M. Carriere, L. Sanche, C. Sicard-Roselli, *Radioprotection* **43** No 5, 185 (2008). DOI:
9. F. Shikata, H. Tokumitsu, H. Ichikawa, Y. Fukumori, *Eur. J. Pharmac. Biopharmac.* **53**, 57 (2002).
10. E.M. Hébert, P.J. Debouttière, M. Lepage, L. Sanche, D.J. Hunting, *Int. J. Radiat. Biol.* **86** No 8, 692 (2010).
11. G. Le Duc, I. Miladi, C. Alric, P. Mowat, E. Bräuer-Krisch, A. Bouchet, E. Khalil, C. Billotey, M. Janier, F. Lux, T. Epicier, P. Perriat, S. Roux, O. Tillement, *ACS Nano* **5** No 12, 9566 (2011).
12. I. Miladi, G.L. Duc, D. Kryza, A. Berniard, P. Mowat, S. Roux, J. Taleb, P. Bonazza, P. Perriat, F. Lux, O. Tillement, C. Billotey, M. Janier, *J. Biomater. Appl.* **28** No 3, 385 (2013).
13. M. Rogosnitzky, S. Branch, *Biometals* **29**, 365 (2016).
14. V. Granata, M. Cascella, R. Fusco, N. Dell'Aprovitola, O. Catalano, S. Filice, V. Schiavone, F. Izzo, A. Cuomo, A.A. Petrillo, *Biomed. Res. Int.* **2016** No 1, 3918292 (2016).
15. Y. Cao, L. Xu, Y. Kuang, D. Xiong, R. Pei, *J. Mater. Chem. B* **5**, 3431 (2017).
16. R. Marasini, T.D. Thanh Nguyen, S. Aryal, *Wiley Interdiscip. Rev. Nanomed. Nanobiotechnol.* **12** No 1, e1580 (2019).
17. P. Šimečková, F. Hubatka, J. Kotouček, P. Turánek Knötigová, J. Masek, J. Slavík, O. Kovác, J. Neca, P. Kulich, D. Hrebík, J. Stráská, K. Pencíková, J. Procházková, P. Divis, S. Macaulay, R. Mikulík, M. Raska, M. Machala, J. Turánek, *Sci. Rep.* **10**, 4780 (2020).
18. F. Benlakdar, A.S.A. Dib, A.H. Belbachir, *Radioprotection* **51** No 4, 279 (2016).
19. A.D. Paro, M. Hossain, T.J. Webster, M. Su, *Int. J. Nanomed.* **11**, 4735 (2016).
20. C. Noblet, G. Delpon, S. Supiot, V. Potiron, F. Paris, S. Chiavassa, *Radiation Oncology* **13**, 32 (2018).
21. J.W. Seo, J.C. Ang, L.M. Mahakian, S. Tam, B. Fite, E.S. Ingham, J. Beyer, J. Forsayeth, K.S. Bankiewicz, T. Xu, K.W. Ferrara, *J. Control. Release.* **220**, 51 (2015).
22. *Methods in Molecular Biology 1741; Glioblastoma: Methods and Protocols (1ed.)* (Ed. by D.G. Placantonakis) (2018).
23. E. Boisseliera, D. Astruc, *Chem. Soc. Rev.* **38**, 1759 (2009).
24. M. Yamada, M. Foote, T.W. Prow, *Wiley Interdiscip. Rev.: Nanomed. Nanobiotechnol.* **7** No 3, 428 (2015).
25. S.H. Lee, B.H. Jun, *Int. J. Mol. Sci.* **20** No 4, 865 (2019).
26. C. Verry, L. Sancey, S. Dufort, G. Le Duc, C. Mendoza, F. Lux, S. Grand, J. Arnaud, J.L. Quesada, J. Villa, O. Tillement, J. Balosso, *BMJ Open* **9** No 2, e023591 (2019).
27. N. Mauro, R. Cillari, C. Gagliardo, M.A. Utzeri, M. Marrale, G. Cavallaro, *ACS Appl. Nano Mater.***6** No 18, 17206 (2023).
28. S.K. Singh, M.K. Singh, P.P. Kulkarni, V.K. Sonkar, J.J.A. Grácio, D. Dash, *ACS Nano* **6** No 3, 2731 (2012).
29. S. Agostinelli, J. Allison, K. Amako, J. Apostolakis, H. Araujo, P. Arce, M. Asai, D. Axen, S. Banerjee, G. Barrand, F. Behner, L. Bellagamba, J. Boudreau, L. Broglia, A. Brunengo, H. Burkhardt, S. Chauvie, J. Chuma, R. Chytracek, G. Cooperman, D. Zschiesche, *Nucl. Instrum. Meth. Phys. Res. A* **506** No 3, 250 (2003).
30. S. Incerti, B. Suerfu, J. Xu, V. Ivantchenko, A. Mantero, J.M.C. Brown, M.A. Bernal, Z. Francis, M. Karamitros, H.N. Tran, *Nucl. Instrum. Meth. Phys. Res. B* **372**, 91 (2016).
31. L. Pandola, C. Andenna, B. Caccia. *Nucl. Instrum. Meth. Phys. Res. B* **350**, 41 (2015).
32. S. Chauvie, S. Guatelli, V. Ivanchenko, F. Longo, A. Mantero, B. Mascialino, *IEEE Symposium Conference Record Nuclear Science* **3**, 1881 (2004).
33. D.R. White, R.V. Griffith, I.J. Wilson, *Reports of the International Commission on Radiation Units and Measurements* **24** No 1, 5 (1992).
34. P.A.P. Moran, *Biometrika* **62** No 1, 1 (1975).
35. M. Santibáñez, Y. Guillen, D. Chacón, R. G. Figueroa, M. Valente, *Appl. Radiation Isotope.* **141**, 210 (2018).
36. A. Ku, V.J. Facca, Z. Cai, R.M. Reilly, *EJNMMI Radiopharm. Chem.* **4**, 27 (2019).
37. K. Haume, S. Rosa, S. Grellet, M.A. Śmiałek, K.T. Butterworth, A.V. Solov'yov, K.M. Prise, J. Golding, N.J. Mason, *Cancer Nanotechnol.* **7**, 8 (2016).
38. S. Hashemi, S.M.R. Aghamiri, R. R. Jaberi, Z. Siavashpour, *Brachytherapy* **20** No 2, 420 (2021).

Наночастинки гадолінію: перспективний агент для посилення радіотерапії при низьких концентраціях

L. Benabed[1], A.S.A. Dib[1], A. Djelloul[2]

[1] *Departement of Physics, Faculty of Physics, Laboratory of Analysis and Application of Radiation, Université des Sciences et de la Technologie d'Oran Mohamed Boudiaf, USTO-MB, BP 1505 EL M'naouer, 31000 Oran, Algeria*
[2] *Centre de Recherche en Technologie des Semi-Conducteurs pour l'Energétique 'CRTSE', 02 Bd Frantz Fanon, BP 140, 7 Merveilles, Alger, Algérie*

Протягом останніх кількох років наномедицина досягла значного прогресу. Наночастинки зараз вводяться в пухлини для покращення лікування, підвищення ефективності доставки ліків до пухлин та зниження токсичності методів лікування раку. Метою цієї роботи є дослідження покращення стану глибокої пухлини в центрі голови людини за допомогою променевої терапії, при якій наноматеріали вводилися в невеликих кількостях. Використовуючи код Монте-Карло Geant4, ми побудували геометрію людської голови, в яку помістили сферичну пухлину діаметром 1,3 см. Нас цікавить дослідження впливу біосумісних наноматеріалів, доданих до пухлин під час рентгенівської променевої терапії. Ми зосередилися на найвідоміших біосумісних наноматеріалах, що використовуються в наномедицині,

включаючи гадоліній (GdNPs), платину (PtNPs), срібло (SvNPs) та золото (AuNPs), особливо при низьких концентраціях. Наші результати показують, що, порівняно з іншими наноматеріалами, присутність GdNPs всередині пухлини забезпечує найбільше поглинання дози на рівні пухлини при впливі рентгенівського випромінювання з енергією 60 кеВ, з ефективністю 37 %. Порівняно з найвідомішими матеріалами в літературі, такими як золото та платина, наше моделювання методом Монте-Карло демонструє, що наночастинки гадолінію мають високу ефективність при низьких концентраціях.

Ключові слова: Доза опромінення, Наноматеріали, Ефект Оже, Поглинання дози пухлиною, Тривимірна топографія поверхні.